HHS Public Access

Author manuscript

Clin Cancer Res. Author manuscript; available in PMC 2018 March 15.

Published in final edited form as:

Clin Cancer Res. 2017 September 15; 23(18): 5446–5459. doi:10.1158/1078-0432.CCR-17-0342.

Patient-derived interstitial fluids and predisposition to aggressive sporadic breast cancer through collagen remodeling and inactivation of p53

Timothy Kenny[1], **Hank Schmidt, MD PhD**[2,3], **Kerin Adelson, MD**[2], **Yujin Hoshida, MD PhD**[4], **Anna P. Koh**[4], **Nagma Shah**[1], **John Mandeli, PhD**[5], **Jess Ting, MD**[3], and **Doris Germain, PhD**[1]

[1]Tisch Cancer Institute, Division of Hematology and Medical Oncology of the Icahn School of Medicine at Mount Sinai, New York, New York 10129

[2]Tisch Cancer Institute, Dubin Breast Center of the Icahn School of Medicine at Mount Sinai, New York, New York 10129

[3]Tisch Cancer Institute, Department of Surgery of the Icahn School of Medicine at Mount Sinai, New York, New York 10129

[4]Tisch Cancer Institute, Department of Medicine of the Icahn School of Medicine at Mount Sinai, New York, New York 10129

[5]Department of Biostatistics of the Icahn School of Medicine at Mount Sinai, New York, 10129 New York

Abstract

Background—Despite the fact that interstitial fluid (IF) represents a third of our body fluid, it is the most poorly understood body fluid in medicine. Increased IF pressure is thought to result from the increased deposition of extracellular matrix in the affected tissue preventing its reabsorption. In the cancer field, increased rigidity surrounding a cancerous mass remains the main reason that palpation and radiological examination, such as mammography, are used for cancer detection. While the pressure produced by IF has been considered, the biochemical composition of IF has not been considered in its effect on tumors.

Methods—We classified 135 IF samples from bilateral mastectomy patients based on their ability to promote the invasion of breast cancer cells.

Results—We observed a wide range of invasion scores. Patients with high-grade primary tumors at diagnosis had higher IF invasion scores. In mice, injections of high-score IF (IF^{High}) in a normal mammary gland promotes ductal hyperplasia, increased collagen deposition, and local invasion. In a mouse model of residual disease, IF^{High} increased disease progression and promoted aggressive visceral metastases. Mechanistically, we found that IF^{High} induces myofibroblast differentiation and collagen production through activation of CLIC4. IF^{High} also down-regulates RYBP, leading to degradation of p53. Further, in mammary glands of heterozygous p53-mutant knock-in mice, IF^{High} promotes spontaneous tumor formation.

Conclusions—Our study indicates that IF can increase the deposition of extracellular matrix and raises the provocative possibility that they play an active role in the predisposition, development, and clinical course of sporadic breast cancers.

Introduction

Interstitial fluid (IF) originates from the blood and infiltrates tissues where it occupies all extra-cellular space to eventually be reabsorbed by the lymph nodes (1,2). Studies of IF have mainly focused on the imbalance of its cycling, as this results in increased pressure in specific tissues and causes diseases such as glaucoma, lymphedema, and intracranial pressure. The increased IF pressure is thought to result from the increased deposition of extracellular matrix in the affected tissue preventing its reabsorption (2). In the cancer field, increased rigidity surrounding a cancerous mass remains the main reason that palpation and radiological examination, such as mammography, are used for cancer detection (3).

The potential role of IF in cancer, which is in direct contact with malignant cells, has not been considered. One major difficulty in the study of IF is its collection. The post-surgical fluids (PSF) collected from surgical drains represent an option to circumvent this difficulty. However, one pitfall is that in addition to the interstitial fluid, PSF reflect a wound healing response and contain several inflammatory cytokines, which are linked to tumorigenesis (4–6). Several studies reported an alarming pro-tumorigenic effect of these PSF, leading to the conclusion that surgery may promote recurrence (7–9). However, since these studies did not differentiate the effect of IF versus surgery-induced inflammation, this conclusion may be misleading. Additionally, in these studies, PSF were collected from unilateral mastectomys, raising the possibility that the composition of the fluid may also be altered by the prior presence of a tumor in the affected breast. In agreement with this possibility, several studies have focused on tumor interstitial fluid composition (10–13). To account for these difficulties, we initiated a study where we collected PSF from patients undergoing bilateral mastectomy for the treatment of unilateral breast cancer. All fluids were tested for their ability to promote cancer cell invasion. In addition, to differentiate the effect of the IF component of PSF from the surgery-induced inflammation component of the PSF, we examined whether a correlation existed between clinical characteristics of the tumor and the biological activity of the fluids.

The results indicate that exposure of a breast to a pro-invasive IF, long before surgery and therefore independentd of surgery-induced inflammation, predisposes an individual to develop more aggressive breast cancer and promotes the formation of a desmoplastic stroma. Mechanistically, we show that altered collagen deposition and inactivation of the tumor suppressor p53 collaborate to mediate the effect of pro-invasive IF on breast cancer cells.

Materials and Methods

Post-Surgical Fluid (PSF)

PSF was obtained from Jackson-Pratt drains placed in the breast or abdomen of women treated for breast cancer at Mount Sinai Hospital. PSF was collected at 24 and 48 hours after mastectomy by plastic surgery service and sterilized using a 0.22 μm pore filter (Millipore).

Patient Demographic, Clinical, & Pathological Characteristics

Under an IRB approved protocol, patient charts were reviewed to collect demographic, clinical, and pathological characteristics of our patient cohort. Invasion score of PSF sample derived from diseased breast at 24 hours post-operatively (post-op) was compared to the invasion score of PSF sample derived from benign breast at 24 hours post-op of the same patient using a Wilcoxin Matched-Pairs Signed Rank test. In addition to reported *p* value, Spearman correlation coefficient (rs) was calculated. The highest invasion score of PSF samples collected 24 hours post-op from either breast of a given patient was compared to invasion score from PSF sample collected from abdomen of the same patient at both 24 and 48 hours post-op in the same patient with separate Wilcoxin Matched-Pairs Signed Rank tests. Lastly, invasion score from PSF samples obtained from the abdomen at 24 and 48 hours post-op in a given patient was compared using a Wilcoxin Matched-Pairs Signed Rank test. Univariate analysis was completed on all collected demographic, clinical, and pathologic patient characteristics with respect to invasion score of PSF sample derived from diseased breast 24 hrs. post-op, treated as a continuous variable, using correlation analysis, Mann Whitney test, or unpaired t-test with Welch's correction, as applicable.

Cell Culture

MDA-MB-231, MDA-MB-157, HBL-100, and MCF7 cells were cultured in Delbecco's modified eagle medium (DMEM) supplemented with 10% fetal bovine serum (FBS) and 100 units/mL Penicillin/Streptomycin (P/S) (Gibco). Primary human mammary fibroblasts (HMF) were purchased from ScienCell and cultured on poly-D-lysine in fibroblast medium supplemented with 2% FBS, 1% fibroblast growth serum (FGS), and 100 units/mL P/S according to manufacturer guidelines (ScienCell). HER2 murine mammary carcinoma cells were derived from MMTV-rtTA/TetO/NeuNT mice and cultured in DMEM/F-12 with GlutaMAX (Gibco) supplemented with 10% fFBS, 100 units/mL P/S (Gibco), 0.25 μg/mL Amphotericin B (Gibco), 25 ng/mL Hydrocortisone (Sigma-Aldrich), and 2 μg/mL Doxycycline hyclate (Sigma-Aldrich). All cell culture was done at 37°C and 5% CO_2.

Human Mammary Fibroblast (HMF) Treatment with PSF

Twenty-four hours after plating HMF in complete media as described above, cells were washed with PBS and serum-starved for 24 hrs in fibroblast media supplemented with 100 units/mL P/S. Following serum-starvation, cells were given fibroblast media supplemented with 100 units/mL P/S and 1% PSF (4 independent high score PSF samples and 4 independent low score PSF samples were used) and cultured for 24 hrs and subsequently collected by trypsinization for western blot analysis.

Invasion Assay

A transwell in vitro invasion assay was used to quantify and characterize the ability of PSF to induce cell migration and invasion. Growth factor reduced matrigel basement membrane matrix (BD Biosciences) was diluted 1:100 in cold PBS and 200 μL was added to the top of the cell permeable membrane (0.3 μm pore size) inside the cell culture inserts for 24 well plates (Falcon). These inserts were then incubated at room temperature for 2 hours. Cells were trypsinized, collected, and seeded atop matrigel coated filters in respective serum free

media depending cells used, as described above. Patient PSF samples were diluted 1:100 in respective serum free and used as the chemoattractant in the bottom chamber. All patient PSF samples were run in at least triplicate and invasion assay was incubated at at 37°C and 5% CO_2 for 48 hours. Following incubation period, invading cells attached to the exterior side of the cell culture insert were fixed and stained using the Hema 3 Manual Staining Stat Pack according to manufacturer guidelines (Fisher Scientific). To calculate invasion score in MDA-MB-231 invasion assays using all patient PSF samples, an image was then taken of each membrane at 4× objective using a Nikon Eclipse Ci-E light microscope and the number of nuclear pixels was calculated using ImageJ. This value was dived by total pixel area and multiplied by 100 to yield an invasion score.

In Vitro Proliferation Assay

One thousand MDA-MB-231 cells were plated in a 24-well plate in complete media. Twenty-four hours after seeding, cells were washed with PBS and serum starved for 24 hours. Following serum starvation, cells were treated with FBS-free media supplemented with 100 units/mL P/S and either 1% high Score PSF, 1% low Score PSF, or 1% FBS. Proliferation was assessed at indicated time points. MTT ((3-(4,5-Dimethylthiazol-2-yl)-2,5-Diphenyltetrazolium Bromide) (Sigma) was used at concentration of 0.5 mg/mL and absorbance read at 570nM to assess the proliferation of cells.

Murine Experiments

Female nude mice aged 4–6 weeks were purchased from Jackson Laboratory. To assess the impact of PSF on the normal mammary gland, 1% PSF was injected subcutaneously into the left and right thoracic and inguinal mammary fat pads of the mice. Mice were treated with 1% PSF (derived from tumor breast of mastectomy patients 24 hours post-surgery; 4 independent high score PSF samples and 4 independent low score PSF samples were used in separate mice) in FBS-free DMEM supplemented with 100 units/mL P/S (Gibco) for a total of three times at intervals of 72 hours. Seventy-two hours following final 1% PSF injection, mice were harvested.

To assess the impact of PSF on residual disease growth and facilitation of local invasion and distant metastasis, 1×10^6 MDA-MB-231 cells in 100 μL of either 100% growth factor reduced matrigel basement membrane matrix (BD Biosciences) or 50% collagen type one (3.12 mg/mL, rat tail, Corning), 50% growth factor reduced matrigel basement membrane matrix (BD Biosciences) was injected into the right thoracic and bilateral inguinal mammary fat pads of nude mice. One week following xenograft, 1% PSF (derived from tumor breast of mastectomy patients 24 hours post-surgery; 1 high score PSF sample and 1 low score PSF samples were used in separate mice) in FBS-free DMEM supplemented with 100 units/mL P/S (Gibco) was injected bilaterally in the thoracic and inguinal fat pads. A total of three 1% PSF injections were completed in 72-hour intervals. Tumor growth was measured weekly using electronic calipers (VWR) and volume was calculated (Length × Width^2 × 0.5).

The $p53^{515A}$ knock-in mice were obtained from Dr. Gigi Lozano's laboratory and 1% PSF was injected subcutaneously into the left and right thoracic and inguinal mammary fat pads of the mice. Mice were treated with 1% PSF (derived from tumor breast of mastectomy

patients 24 hours post-surgery; 1 high score PSF sample was used on one side of the mouse and 1 low score PSF sample was used on the other side of the mice) in FBS-free DMEM supplemented with 100 units/mL P/S (Gibco) for a total of three times at intervals of 72 hours. Seventy-two hours following final 1% PSF injection, mice were harvested. All samples were either snap frozen for protein and RNA extraction or fixed in 10% Formalin (Fisher Scientific) for paraffin-embedded sections.

Masson's Trichrome Stain and Collagen Quantification

Paraffin embedded slides were deparaffinized in xylene and rehydrated in water. Sections were then placed in Bouin's fluid (Picric acid, 40% formalin, glacial acetic acid) in a 56 °C water bath for 1 hour. Slides were then incubated in Weigert's iron hematoxylin stain for 10 minutes, Biebrich scarlet-acid fuchsin solution for 7 minutes, phosphotungstic-phosmolybdic acid solution for 5 minutes, and analine blue stain solution for 7 minutes, all at room temperature with washes completed in deionized H_2O (Dako). Slides were then differentiated in 1% acetic acid solution for 1 minute and mounted with Permount toluene solution (Fisher Scientific). For quantification, collagen signal area was measured in images taken with a Zeiss AX10 light microscope at 10× objective (Zeiss) by manually selecting regions positive for collagen, in Adobe Photoshop and quantified using ImageJ.

Second Harmonic Generation (SHG) Imaging

SHG imaging was completed at the Microscopy Core Facility at The Icahn School of Medicine at Mount Sinai. Images were captured using the Olympus SV1000MPE Multiphoton Flouview multiphoton laser scanning microscope operated with Olympus Flouview software. The microscope was fitted with a Coherent Chameleon Vision II TiS laser with a 680–1080 nm tuning range, dispersion compensation, and 140 femtosecond pulse width and was equipped with a 25× XLPlanN water immersion multiphoton objective lens (NA = 1.05; Olympus). Laser excitation was controlled using an acousto-optic modulator under managed through the Flouview software. Using 860 nm incident excitation light, SHG signal was captured using a 420–460 nm bandpass filter, a 485 dichroic mirror (GR/XR filter cube, Olympus), and a non-descanned (external) detector, as has been previously described (14).

Tumor-associated Collagen Signature (TACS) Identification in SHG Imaging

Collagen alignment relative to the border of mammary ducts treated with PSF was analyzed in SHG obtained images using the curvelet-based alignment analysis software, CurveAlign, available through the Laboratory of Optical and Computational Instrumentation at the University of Wisconsin-Madison. SHG images were imported into the CurveAlign software and the tips of mammary ducts were outlined. CurveAlign software was used to identify the angle of collagen fibers with the outlined interface within a preset pixel distance. The angle of interaction of individual collagen fibers was reported as an output value between 0 and 90. Angles of interaction were binned into four categories: 0–20°, 20–40°, 40–60°, and 60–90°. The number of individual collagen fibers having an angle of interaction within the four categories were counted and normalized to the total number of collagen fibers assessed by the software. The percentage of fibers assessed having an angle of interaction of 60–90° in

multiple quantifications in different fields were compared between PSF treatments using an unpaired two-sided t-test.

Microarray and Analysis

Twenty-four hours after plating MDA-MB-231 cells in complete media as described above, cells were washed with PBS and serum-starved for 24 hrs in DMEM supplemented with 100 units/mL P/S. Following serum-starvation, cells were given DMEM media supplemented with 100 units/mL P/S and 1% PSF (derived from tumor breast of mastectomy patients 24 hours post-surgery; 4 independent high score PSF samples and 4 independent low score PSF samples were used) and cultured for 24 hrs and subsequently collected by trypsinization for RNA extraction. As a control, one plate of MDA-MB-231 cells was treated with complete media (10%FBS supplemental with 100 units/mL P/S) for 24 hrs following 24 hrs of serum starvation, though this was not analyzed in the microarray but was used for rt-PCR analysis. RNA was extracted from MDA-MB-231 treated cells with PSF using the RNeasy Mini Kit according to manufacturer's guidelines (Qiagen). RNA samples were sent to the Genomics Core Facility at the Icahn School of Medicine at Mount Sinai where microarray analysis was performed. Raw expression data was obtained from the core facility and subsequently normalized and filtered for variation. Gene expression was compared between high score and low score PSF treated cells using ComparativeMarkerSelection and Gene Set Enrichment Analysis (GSEA) available through GenePattern (Broad Institute). The 1000 most differentially expressed genes between high score PSF samples and low score PSF treated samples (500 upregulated, 500 downregulated in high score vs. low score groupings) were analyzed using Enrichr, a gene list enrichment analysis tool (15,16).

Quantitative Real-Time Polymerase Chain Reaction (rt-PCR)

Quantitative rt-PCR was performed with 100 ng of RNA in 20 μL per assay well using the PrimeScript One Step RT-PCR kit (Takara/Clontech). The reaction was performed with the DNA Engine Opticon System (Bio-Rad) under conditions recommended by the manufacturer. Expression levels were normalized to that of Actin and the following primers used: human CLIC4 forward (5′-GGTGATTCTGAACCTTGCCTCA-3′), human CLIC4 reverse (5′ TCCTCTTGTTAGCCCTCCACCT-3′), human RYBP forward (5′-TTTGCC CAGAAAGACAGCTT-3′), human RYBP reverse (5′ GTCGTGCACATGCCAGTAAC-3′), human β Actin forward (5′-ATCCTCACCCTGAAGTACCC-3′), human β Actin reverse (5′-TAGAAGGTGTGGTGCCAGAT-3′).

Western Blot

MDA-MB-23, HMF, or murine mammary glands cells were lysed in NP40 Lysis Buffer (50 mM Tris, pH 7.5, 250 mM NaCl, 5 mM EDTA, 0.5% Nonidet P-40, 50 mM NaF, 0.2 mM Na_3VO_4, 1 mM DTT, 10 mg/mL luepeptin, 1.74 mg/mL PMSF, 1 mg/mL pepstatin A) and clarified by centrifugation at 4 °C for 20 minutes at 14,000 rpm. Protein concentration was measured using the Bradford method (BioRad). Proteins were separated by SDS-Page electrophoresis, transferred to nitrocellulose membrane (GE Health), and probed with alpha smooth muscle actin (mouse, Sigma-Aldrich), GAPDH (mouse, EMD Millipore), p53 (DO1

mouse, Santa-Cruz), p21 (C19 rabbit, Santa Cruz), IGFBP5 (rabbit, EMD Millipore), and Actin (mouse, EMD Millipore).

Immunohistochemistry

For immunostaining of parrafin-embedded sections with alpha smooth muscle actin (mouse, Sigma-Aldrich), sections were deparaffinized in xylene, rehydrated in water, and antigen retrieval was performed in citrate buffer. Endogenous peroxidase activity was blocked with 3% hydrogen-peroxide solution for 10 minutes. Serum blocking was performed for 10 minutes prior to incubation with alpha smooth muscle actin at 1:400 dilution for 1 hour at room temperature. Secondary antibody was incubated for 30 minutes at room temperature and then developed using a LAB-SA peroxidase kit for 3 minutes (Invitrogen). All washes were performed with tris-buffered saline (TBS) three times for 2 minutes.

Cytokine Array

Human Cytokine Array C5 (RayBiotech) was used according to manufacturer guidelines to assess the presence of cytokines in 8 different PSF samples which were analyzed after diluting 1:3 in provided buffer.

Results

Classification of PSF according to breast cancer cells invasion score

We collected PSF from a total of 46 patients at either 24 hours or both 24 and 48 hours after surgery. Each PSF was tested in triplicate by invasion assay using the triple negative breast cancer cell line MDA-MB-231 and an invasion score (IS) was calculated. The distribution of the invasion scores is shown in Figure 1A. Representative images of various invasion scores are shown in Figure 1B. Initially, only PSF from bilateral mastectomy patients treated for unilateral breast cancer were collected to allow the direct comparison between the PSF derived from the diseased-breast (tumor-breast) and the normal breast taken prophylactically. No significant difference was observed between the invasion score of the two breasts from the same individual (Fig. 1C, D), indicating that the prior presence of the tumor did not affect the invasion score. Based on this result, we subsequently extended our collection to patients undergoing unilateral mastectomy. As a result, 72% of PSF were collected from bilateral mastectomy patients and 28% were collected from unilateral mastectomy patients (Fig. 1E). Of the 46 patients, 17 also had autologous reconstruction (Fig. 1E) allowing for the direct comparison of the PSF derived from their abdomen and their breasts. We found a statistically significant difference between the invasion score of the breast-derived PSF relative to the abdomen-derived PSF at the same time point from the same patient (Fig. 1F). As inflammation and wound healing is a common denominator of all surgical sites, this result is the first indication that surgery-induced inflammation alone is not the major determinant of the invasion score. This result also suggests that the interstitial fluid (IF) component of the PSF rather than inflammation component of the PSF is the driver of the invasion. Further, this result indicates that fluids from different anatomical areas of the same individual show differences in their ability to promote the invasion of cancer cells. For some patients, PSF were collected at both 24 and 48 hours after surgery, allowing for the comparison of invasion scores of PSF from the same breast at both time points.

Except for a few cases, the invasion score increased significantly at 48 hours compared to 24 hours (Fig. 1G), indicating increased invasion capacity. However, as samples at 24 hours were collected for all patients but only a subset of patients were also collected at 48 hours, the samples collected at 24 hours were used for all subsequent analysis.

Retrospective analysis of PSF invasion score and clinical features

The clinical parameters collected from medical charts for all 46 patients in the study are shown in figures 2A, and 2B. Given that obesity is linked to chronic inflammation (14), we reasoned one trivial explanation for our results may be body mass index (BMI). However, no significant correlation between BMI and PSF invasion score was observed (Fig. 2C). Of all clinical correlates analyzed for a potential link with PSF invasion scores, only three showed statistical significance. We found that patients diagnosed with 1) grade 3 (poorly differentiated) breast cancer (Fig, 2D), 2) 1 or more positive lymph nodes (Fig. 2E) and 3) estrogen receptor (ER) negativity (Fig. 2F) were associated with higher invasion score PSF. Therefore, high score PSF retrospectively identified patients diagnosed with more aggressive primary breast cancers. As the analysis of PSF from both the diseased breast and the normal breast show the same score within an individual patient, this result supports the notion that the IF component of the PSF may be an intrinsic characteristic of the individual rather than a characteristic of their disease. Consequently this result suggests that exposure of the breast to high score IF predisposes the breast to the development of high grade, invasive, ER negative breast cancer.

Effects of low and high score PSF on normal mammary gland

To test experimentally the possibility that exposure to high score IF may predispose a normal breast to more aggressive cancer, we injected high and low score PSF in the mammary fat pad of nude mice. First, to ensure that the effect on invasion were observed on human breast cancer cells is not due to species-specific PSF-derived factors, we repeated the invasion assay on mouse cancer cells derived from inducible erbB2 tumors. We found that high score PSF also promotes the invasion of these cells compared to low score PSF therefore ruling out species-specific effect (Suppl. Fig. 1). In this experiment, mammary fat pads were injected every three days for 3 consecutive times and the mammary glands harvested 3 days after the last injection. We found that injections with low score PSF had no significant effect on the morphology of the mammary ducts (Fig. 3A). However, hyperplasia of the mammary ducts was observed in fat pads injected with high score PSF (Fig. 3B). Notably, hyperplasia was more pronounced at the tip of the ducts. Further, we also tested for the deposition of extracellular matrix proteins using Masson’s Trichome staining for collagen. We found a striking elevation in the deposition of collagen in mammary glands injected with high score PSF but not low score PSF (Fig. 3A–B). Further, the deposition of collagen was also localized to the tip of the mammary ducts.

The spatial distribution of these effects is reminiscent of terminal end buds (TEB), which are the sites of mammary duct growth and invasion trhrough the stroma during puberty. Importantly, the collagen at TEB is characterized by a realignment of the collagen fibers with radial rather than parallel orientation of fibers relative to the ductal edge. Such realignment of collagen normally observed during mammary gland development, is a

process that is also found in breast cancer. This phenomenon is referred as tumor associated collagen signature (TACS) (15). Classification of TACS is based on the angle of collagen fibers to a border. TACS-3 refers to a tumor where the majority of collagen fibers show an angle of 60 to 90° relative to the tumor border. TACS-3 has been reported to be an independent prognostic factor of worse outcome (15). Further, sites of TACS-3 were shown to facilitate the invasion of cancer cells into the stroma. TACS can be quantified using second harmonic generation microscopy (16). We therefore performed second harmonic generation imaging on mammary glands injected with low or high score PSF and found a significant increase in TACS3 in mammary glands injected with high score PSF (Fig. 3D–E–F).

Therefore, these results show that high score PSF induces epithelial hyperplasia and invasion in addition to collagen deposition and the formation of TACS-3.

Effects of low and high score PSF on residual disease

As the PSF were classified based on their ability to promote the invasion *in vitro* using MDA-MB-231 cells, we postulated that this effect may be reproduced *in vivo*. To mimic the post-surgical scenario of a breast where some cancer cells remain and are exposed to this fluid, we used smaller number of cells normally used in mice to form a tumor and followed the same protocol and schedule of injections of PSF as above, one week after xenoengraftment of MDA-MB-231 cells. We then monitored tumor formation over a period of 8 weeks. We found that MDA-MB-231 cells did not significantly grow in mice injected with the low score PSF, as the volume did not appreciably increase over time (Fig. 4A, B). In mice injected with the high score PSF, however, tumor volumes increased over time and were significantly larger than the low score treated tumors (Fig. 4A, B). To test the possibility that low score fluids inhibit the growth of cells, we monitored the effect of high and low score fluids relative to cells that were treated with 1% fetal bovine serum (FBS) *in vitro*. We found that while high score fluid promoted growth relative to low score fluids, low score fluid treated cells grew significantly better than those treated with 1% FBS (Suppl. Fig. 2). Therefore, we concluded that low score PSF does not inhibit growth. Further, upon histological analysis of the tumors in each group, we found that tumors in the low score PSF group were well circumscribed and showed necrosis (Fig. 4C). However, tumors in the high score PSF showed diffused margins and were highly cellular (Fig. 4D). Therefore, high score PSF promotes proliferation as well as local invasion in a model of residual disease.

As we found that high score PSF promotes the deposition of collagen, we postulated that the number of cells injected may exceed the amount of collagen produced by the short period of injections and therefore constrain metastatic behavior, so we repeated the same experiment using a supplement of collagen. Under these conditions, we found that cells exposed to low score PSF grew significantly larger (Fig. 4E, F, blue line) than in absence of collagen (Fig. 4A, red line). In contrast the tumor volumes in the high score PSF group were smaller (Fig. 4E, F). However, tumors exposed to low score fluids remained necrotic while those exposed to high score fluids were highly cellular (Fig. 4G).

To investigate the possibility that the smaller and highly cellular primary tumors exposed to the high score fluid may have increased invasion, we monitored surrounding tissues for

metastases. We found massive visceral metastases in 40% of the mice injected with high score fluids, while no metastases were observed in the mice exposed to low score fluids (Fig. 4H, I). Further, while the MDA-MB-231 cells are known to be invasive using invasion chamber assay and metastasis to the lung using tail vein injections, these cells do not normally induce visceral metastases from a primary site. These results therefore confirm the proliferative and invasive effects of high score PSF and further indicate that collagen plays a key role in this process.

Up-regulation of CLIC4 and down-regulation of RYBP contribute to the differential effects of low and high score PSF

In order to understand the mechanistic basis of the results we observed *in vitro* and *in vivo*, we performed a microarray analysis on MDA-MD 231 cells treated with eight independent low or high score PSF samples. Unbiased hierarchical clustering revealed a clear genetic signature that distinguishes high from low score PSF treated samples. The 50 most differentially expressed genes between the two groups are shown in a heat map (Fig. 5A). Pathway analysis revealed that focal adhesion and cell-substrate junctions were the most significant cellular components differentially affected by PSF treatment (Fig. 5B). This analysis is consistent with the increase in collagen deposition which we had previously seen in the mammary glands of high score treated mice. Therefore, we first focused on genes implicated in collagen deposition. CLIC4 is one the top up-regulated genes in MDA-MB-231 by high score PSF. CLIC4 has been identified as the gene most up-regulated in fibroblasts upon exposure to TGF-β1 and was found to be required for the differentiation of fibroblasts to myofibroblasts (17). Considering that myofibroblasts are responsible for the deposition of collagen, CLIC4 is a prime candidate to contribute to the increased deposition of collagen observed upon exposure to high score PSF. As a control, we confirmed that CLIC4 is increased relative to cells that were not treated with PSF (Suppl. Fig. 3)

However, we reasoned that while CLIC4 was identified by microarray analysis on MDA-MB-231 breast cancer cells, *in vivo*, the up-regulation of CLIC4 must be most important in fibroblasts. To test this possibility, we monitored the ability of high score PSF to induce the formation of myofibroblasts using alpha smooth muscle actin (αSMA) as a marker of differentiation since the up-regulation of CLIC4 promotes the differentiation of fibroblasts to myofibroblasts. We treated fibroblasts with high score PSF and found a significant increase in αSMA protein levels in fibroblasts treated with high score PSF (Fig. 5C–D). To further validate this observation, we monitored the presence of myofibroblasts in vivo using immunohistochemistry of αSMA in normal mammary glands treated with high and low score PSF. This analysis confirmed an increase in myofibroblasts in mammary glands treated with high score PSF and most noticeably the elevation in smooth muscle actin correlated with the increase in collagen deposition at the tip of the ducts (Fig. 5E–F). Therefore, this analysis suggests that elevation in CLIC4 contributes to the increased deposition of collagen observed following exposure to high score PSF.

Pathway analysis on the differential gene signature produced by exposure to high or low PSF identified the p53 pathway as the pathway most significantly associated with the PSF gene signature in the PANTHER pathway ontology (Fig. 5G). In addition to collagen deposition,

increased proliferation was also a strong phenotype we observed in the mammary glands treateated with high score PSF. We therefore looked for genes that could link increased proliferation and the p53 pathway. We focused on RYBP, which is one of the most differentially expressed genes in our signature with high expression in the low PSF treated samples and low expression in the high PSF treated samples (Fig. 5A). As a control, we confirmed that RYBP is more highly expressed in cells treated with low score PSF compared to untreated cells (Suppl. Fig 3). Our interest in RYBP arose from the fact that it is normally implicated in the stabilization of the tumor suppressor p53 through its interaction with the ubiquitin ligase mdm2 (18). As we found RYBP is down-regulated by high score PSF, our prediction was that in cells expressing wild-type p53 such as the epithelial cells of normal mammary glands, wild-type p53 levels and its transcriptional targets such as the cdk inhibitor p21 should be also down-regulated. Such deregulation of p53 and the cell cycle would then contribute to the increase in proliferation we observed. To test this possibility, we analyzed the effects of high score fluids on the mammary glands of nude mice. We found that p53 protein levels as well as its target p21 are significantly reduced by independent high score PSF samples (Fig. 5H). This result, therefore, indicates that in addition to abnormal collagen deposition and orientation, treatment with high score PSF leads to the degradation of the tumor suppressor p53 and alters proliferation by decreasing the cdk inhibitor p21.

To further validate the effect of high score PSF on p53, we next turned our attention to the heterozygous mutant $p53^{515A}$-knock-in mice, which express one copy of wild-type p53 and one copy of mutant $p53^{515A}$ (19). As wild type p53 is an established tumor suppressor, more recently gain of oncogenic function of mutant p53 has also been recognized. In human cancers, homozygous loss of wild type p53 is rarely observed, rather, heterozygosity is. Loss of heterozygosity (LOH) involves the loss of the remaining wild-type copy of p53 in the context of a mutation in the second allele. Therefore, this mouse model recapitulates the heterozygosity at the p53 locus that is observed in human. We reasoned that treatment of the mammary gland of these mice with high score PSF would lead to the degradation of wild-type p53 and mimic LOH. If so, our prediction was that the effect of high score PSF may be more drastic in these mice. To test this possibility, we injected heterozygote $p53^{515A}/p53^{wt}$ mice with a low score PSF in the mammary glands on the right side and high score PSF in the mammary glands of the same mice on the left side. Each cycle of injections involved injection on day one followed by two days rest, as was done in all previous murine experiments. Following 3 consecutives cycles of injections, mammary glands were analyzed by histology and western blot. We found that in these mice, some mammary ducts (30%) show dysplasia and hyperplasia in absence of injection of PSF, suggesting that these mice are more prone to proliferation due to the presence of mutant p53 (Fig. 5I). However, the number of abnormal ducts were only slightly increased by injection of low score PSF (38%) (Fig. 5I–J). In contrast, the percentage of abnormal ducts was increased significantly in mammary glands injected with high score PSF (57%) and in addition, 2 spontaneous tumors were observed (Fig. 5I–K). To verify the effect on p53 and p21, we performed a western blot analysis on the mammary glands of the heterozygote $p53^{515A}/p53^{wt}$ mice. A reduction in both was observed (Fig. 5L).

Collectively, our results both *in vivo* and *in vitro* classify PSF as high and low score based on their invasion capacity using the MDA-MD231 cell line. We next aimed at defining

whether this classification holds true in more than one cell lines. We selected three low and three high score PSF and tested their effect on invasion on three additional cell lines. We found that even in non-invasive breast cancer cell lines such as the MCF7 cells, exposure to high score fluid increased significantly their invasion compared to the low score fluids (Fig. 6A). This observation was consistent between cell lines (Fig. 6A).

Having identified CLIC4 on one hand and RYBP on the other hand, we then searched for potential mechanism functionally linking these two pathways. We previously reported that inhibition of IGFBP-5 promotes collagen deposition through the elevation in IGF signaling (20). Further, increased expression of IGFBP-5 during senescence is reported to be p53-dependent (21). In addition, IGFBP-5 prevents TGF-β1 mediated invasion (22). Therefore, we analyzed the levels of IGF binding proteins in the fluids using a cytokine array on which several IGFBP were present. We found that IGFBP1, 3, and 4 were lower in the high score PSF compared to low score PSF (Fig. 6B, C). However, because IGFBP5 is not present in this array, we also analyzed IGFBP-5 by western blot the mammary glands of nude mice treated with either low or high score PSF. We found that IGFBP-5 is significantly down-regulated by high score PSF but not low score PSF (Fig. 6D). This observation suggests that increased IGF-signaling acts as a functional link between the up-regulation of CLIC4 and the down-regulation of RYBP to establish a positive feedback loop between the inhibition of p53 function and increased collagen.

Discussion

The study of interstitial fluids (IF) has been complicated by the inflammatory components of such fluids, as their collection inevitably requires some tissue damage. Results from the analysis of the effect of post-surgical fluids, which contain both IF and inflammatory components, on cancer cells have lead to conclusion that surgery itself may contribute to tumor progression. In contrast however, the results of our retrospective analysis of patient matched PSF samples revealed that patients with high score fluids derived from their breasts, show lower score fluid from the abdomen. This observation indicates that 1) the biological activity of the fluid is not simply the result of inflammation and wound healing from surgery because the abdomen in these patients also underwent surgery, 2) it confirms the observations from other groups that the composition of the interstitial fluid reflects the anatomical environment in which it is derived and that interstitial fluids are organ-specific (2). Further, since the score of the fluids were the same in both breasts from the same patient, we can conclude that the biological activity of the fluid is not affected by the presence of a tumor in the diseased breast. Our interpretation of this finding is that in an individual with high score IF, both breasts are at higher risk of cancer, but these patients will have unilateral disease as a sporadic mutation may happen in one breast and its development enhanced by high score IF.

We found a significant correlation between grade 3, ER negative, and lymph nodes positive tumors with increased PSF invasion score. Since clinically these tumors are already at higher risk of metastasis, one could argue that the presence of high score PSF would not have much impact on post-surgical disease progression. However, since the outcome of xenografts from the exact same cancer cells (MDA-MB-231 cells) exposed to low and high score PSF is

remarkably different, our data suggest that patients with high grade tumors but low score PSF are at lower risk than those with identical high grade tumors and high score PSF. Therefore, analysis of PSF may have prognostic value.

Studies of IF have focused on increased IF pressure due to stiffness of the tumor microenvironment. Our data reveals that interstitial fluid may in fact be an active player in generating the increased stiffness itself by increasing deposition of collagen. We identified CLIC4 as part of the mechanism leading to this effect. In addition, we also identified down-regulation of RYBP as a mechanism to explain the increased proliferation and hyperplasia in normal mammary glands and tumor development in the $p53^{515A}/p53^{wt}$ heterozygous mice. Based on the functions of CLIC4 and RYBP, we propose the model shown in Figures 6E and F, whereby events in the epithelial cells and the stroma cooperate to determine the outcomes of the effects of low and high score PSF. In epithelial cells exposed to low score PSF, RYBP levels are high, leading to a low levels of mdm2 and the stabilization of wild type p53. As a result, cells that acquired abnormalities are detected by p53 checkpoint and eliminated by apoptosis. In addition, the transcription of p53 targets genes such as p21 and IGFBP5 lead to inhibition of the cell cycle and IGF signaling (Fig. 6E). In the stroma of a breast exposed to low score PSF, CLIC4 levels are low and therefore the differentiation of myofibroblasts and production of collagen is low (Fig. 6E).

In epithelial cells exposed to high score PSF, RYBP levels are low leading to elevated levels of Mdm2, which then degrades wild type p53 (Fig. 6F). In absence of p53 the checkpoint is abolished, cells with acquired abnormalities are not eliminated, and the cell cycle is stimulated and proliferation is further promoted by IGF signaling. In the stroma, CLIC4 levels are high and promote the differentiation of fibroblasts into myofibroblasts and the deposition of collagen. While the mechanism by which tumor associated collagen signature (TACS) remains unknown, our data indicate that high score PSF stimulates its formation and work from the Keely group have shown that the presence of TACS is associated with invasion (15,16). Therefore, our data suggest that the combination of the effect of high score fluids on the epithelial cells, fibroblasts and TACS unite several of the conditions favoring aggressive tumor progression and metastasis (Fig. 6F).

While we have focused on the effect of RYBP on p53, it is important to note that RBYP also affects proliferation through its association with E2F6 transcriptional repressor complex (23). Further, RYBP was recently identified as a driver deletion in a whole genome sequencing study (24). Therefore, down-regulation of RYBP also promotes proliferation of cells expressing mutant p53 and is consistent with our finding of the effect of high score PSF on MDA-MB-231 xenografts, which express mutant p53.

Our results raise the intriguing possibility that IF may both predispose to the development of cancer and promote local recurrence and metastasis. Given that the invasion scores of the IF from both the diseased-breast and normal breast within a given patient are the same, it seems that a sporadic mutation in one breast is a requirement for the development of aggressive disease as both breasts are exposed to high score IF. Our data obtained in the $p53^{515A}$ mutant heterozygous mice supports this possibility.

One key unanswered question is what is the source of the difference in the composition of interstitial fluids between individuals? We postulate that familial, environmental, and sporadic events may contribute; however further studies will be required to answer this question.

Collectively, the results indicate that the biological activity of IF is an intrinsic property of an individual. Those with high score fluids are not only at higher risk of developing aggressive breast cancer before surgery, but may also be at higher risk of developing local recurrence and distant metastases after surgery, should residual cancer cells remain. This possibility will be validated in a long-term clinical follow-up study. If indeed the presence of high versus low score PSF at surgery predicts higher risk of metastasis in patients with otherwise identical tumor characteristics, the intent is to use these fluids to complement the current clinical assessment of disease progression by receptors and lymph nodes status. Further, since we found that the high score fluids themselves promote increased extracellular matrix deposition; the possibility that other IF may also do the same in other tissues is raised.

Supplementary Material

Refer to Web version on PubMed Central for supplementary material.

Acknowledgments

We thank Dr. Edgardo Ariztia for sharing his expertise in performing invasion assays. This work was supported by donations from the Anna Maria and Stephen Kellen Foundation, Emad Zikry and Jeffrey Epstein to J. T, by the Samuel Waxman Cancer Research Foundation grant to D.G and by a grant NIH/NIDDK R01 DK099558 Irma T. Hirschl Trust to Y. H.

References

1. Swartz MA, Lund AW. Lymphatic and interstitial flow in the tumour microenvironment: linking mechanobiology with immunity. Nat Rev Cancer. 2012; 12(3):210–9. DOI: 10.1038/nrc3186 [PubMed: 22362216]
2. Wiig H, Swartz MA. Interstitial fluid and lymph formation and transport: physiological regulation and roles in inflammation and cancer. Physiol Rev. 2012; 92(3):1005–60. DOI: 10.1152/physrev.00037.2011 [PubMed: 22811424]
3. Nagelkerke A, Bussink J, Rowan AE, Span PN. The mechanical microenvironment in cancer: How physics affects tumours. Semin Cancer Biol. 2015; 35:62–70. DOI: 10.1016/j.semcancer.2015.09.001 [PubMed: 26343578]
4. Schafer M, Werner S. Cancer as an overhealing wound: an old hypothesis revisited. Nat Rev Mol Cell Biol. 2008; 9(8):628–38. [PubMed: 18628784]
5. Mantovani A, Allavena P, Sica A, Balkwill F. Cancer-related inflammation. Nature. 2008; 454(7203):436–44. DOI: 10.1038/nature07205 [PubMed: 18650914]
6. Valeta-Magara A, Hatami R, Axelrod D, Roses DF, Guth A, Formenti SC, et al. Pro-oncogenic cytokines and growth factors are differentially expressed in the post-surgical wound fluid from malignant compared to benign breast lesions. SpringerPlus. 2015; 4:483.doi: 10.1186/s40064-015-1260-8 [PubMed: 26361584]
7. Tsuchiya Y, Sawada S, Yoshioka I, Ohashi Y, Matsuo M, Harimaya Y, et al. Increased surgical stress promotes tumor metastasis. Surgery. 2003; 133(5):547–55. DOI: 10.1067/msy.2003.141 [PubMed: 12773983]

8. Lee JW, Shahzad MM, Lin YG, Armaiz-Pena G, Mangala LS, Han HD, et al. Surgical stress promotes tumor growth in ovarian carcinoma. Clin Cancer Res. 2009; 15(8):2695–702. DOI: 10.1158/1078-0432.CCR-08-2966 [PubMed: 19351748]
9. Demicheli R, Valagussa P, Bonadonna G. Does surgery modify growth kinetics of breast cancer micrometastases? Br J Cancer. 2001; 85(4):490–2. [PubMed: 11506484]
10. Gromov P, Gromova I, Olsen CJ, Timmermans-Wielenga V, Talman ML, Serizawa RR, et al. Tumor interstitial fluid - a treasure trove of cancer biomarkers. Biochim Biophys Acta. 2013; 1834(11):2259–70. DOI: 10.1016/j.bbapap.2013.01.013 [PubMed: 23416532]
11. Baronzio G, Parmar G, Baronzio M, Kiselevsky M. Tumor interstitial fluid: proteomic determination as a possible source of biomarkers. Cancer genomics & proteomics. 2014; 11(5): 225–37. [PubMed: 25331795]
12. Munson JM, Bellamkonda RV, Swartz MA. Interstitial flow in a 3D microenvironment increases glioma invasion by a CXCR4-dependent mechanism. Cancer Res. 2013; 73(5):1536–46. DOI: 10.1158/0008-5472.CAN-12-2838 [PubMed: 23271726]
13. Gromov P, Gromova I, Bunkenborg J, Cabezon T, Moreira JM, Timmermans-Wielenga V, et al. Up-regulated proteins in the fluid bathing the tumour cell microenvironment as potential serological markers for early detection of cancer of the breast. Molecular oncology. 2010; 4(1):65–89. DOI: 10.1016/j.molonc.2009.11.003 [PubMed: 20005186]
14. Debnath M, Agrawal S, Agrawal A, Dubey GP. Metaflammatory responses during obesity: Pathomechanism and treatment. Obesity research & clinical practice. 2015; doi: 10.1016/j.orcp.2015.10.012
15. Conklin MW, Eickhoff JC, Riching KM, Pehlke CA, Eliceiri KW, Provenzano PP, et al. Aligned collagen is a prognostic signature for survival in human breast carcinoma. Am J Pathol. 2011; 178(3):1221–32. DOI: 10.1016/j.ajpath.2010.11.076 [PubMed: 21356373]
16. Bredfeldt JS, Liu Y, Conklin MW, Keely PJ, Mackie TR, Eliceiri KW. Automated quantification of aligned collagen for human breast carcinoma prognosis. Journal of pathology informatics. 2014; 5:28.doi: 10.4103/2153-3539.139707 [PubMed: 25250186]
17. Shukla A, Edwards R, Yang Y, Hahn A, Folkers K, Ding J, et al. CLIC4 regulates TGF-beta-dependent myofibroblast differentiation to produce a cancer stroma. Oncogene. 2014; 33(7):842–50. DOI: 10.1038/onc.2013.18 [PubMed: 23416981]
18. Chen D, Zhang J, Li M, Rayburn ER, Wang H, Zhang R. RYBP stabilizes p53 by modulating MDM2. EMBO Rep. 2009; 10(2):166–72. DOI: 10.1038/embor.2008.231 [PubMed: 19098711]
19. Lang GA, Iwakuma T, Suh YA, Liu G, Rao VA, Parant JM, et al. Gain of function of a p53 hot spot mutation in a mouse model of Li-Fraumeni syndrome. Cell. 2004; 119(6):861–72. [PubMed: 15607981]
20. Takabatake Y, Oxvig C, Nagi C, Adelson K, Jaffer S, Schmidt H, et al. Lactation opposes pappalysin-1-driven pregnancy-associated breast cancer. EMBO Mol Med. 2016; 8(4):388–406. DOI: 10.15252/emmm.201606273 [PubMed: 26951623]
21. Kim KS, Seu YB, Baek SH, Kim MJ, Kim KJ, Kim JH, et al. Induction of cellular senescence by insulin-like growth factor binding protein-5 through a p53-dependent mechanism. Mol Biol Cell. 2007; 18(11):4543–52. DOI: 10.1091/mbc.E07-03-0280 [PubMed: 17804819]
22. Vijayan A, Guha D, Ameer F, Kaziri I, Mooney CC, Bennett L, et al. IGFBP-5 enhances epithelial cell adhesion and protects epithelial cells from TGFbeta1-induced mesenchymal invasion. Int J Biochem Cell Biol. 2013; 45(12):2774–85. DOI: 10.1016/j.biocel.2013.10.001 [PubMed: 24120850]
23. Trimarchi JM, Fairchild B, Wen J, Lees JA. The E2F6 transcription factor is a component of the mammalian Bmi1-containing polycomb complex. Proc Natl Acad Sci U S A. 2001; 98(4):1519–24. DOI: 10.1073/pnas.041597698 [PubMed: 11171983]
24. Ulz P, Belic J, Graf R, Auer M, Lafer I, Fischereder K, et al. Whole-genome plasma sequencing reveals focal amplifications as a driving force in metastatic prostate cancer. Nature communications. 2016; 7:12008.doi: 10.1038/ncomms12008

Translational relevance

Despite the fact that interstitial fluid (IF) represents a third of our body fluid, it remains one of the most poorly understood and its relevance to cancer is understudied. The results of the current study raise the possibility that IF derived from mastectomy patients may be develop in the future as biomarker to identify breast cancer patients at higher risk of developing metastatic disease.

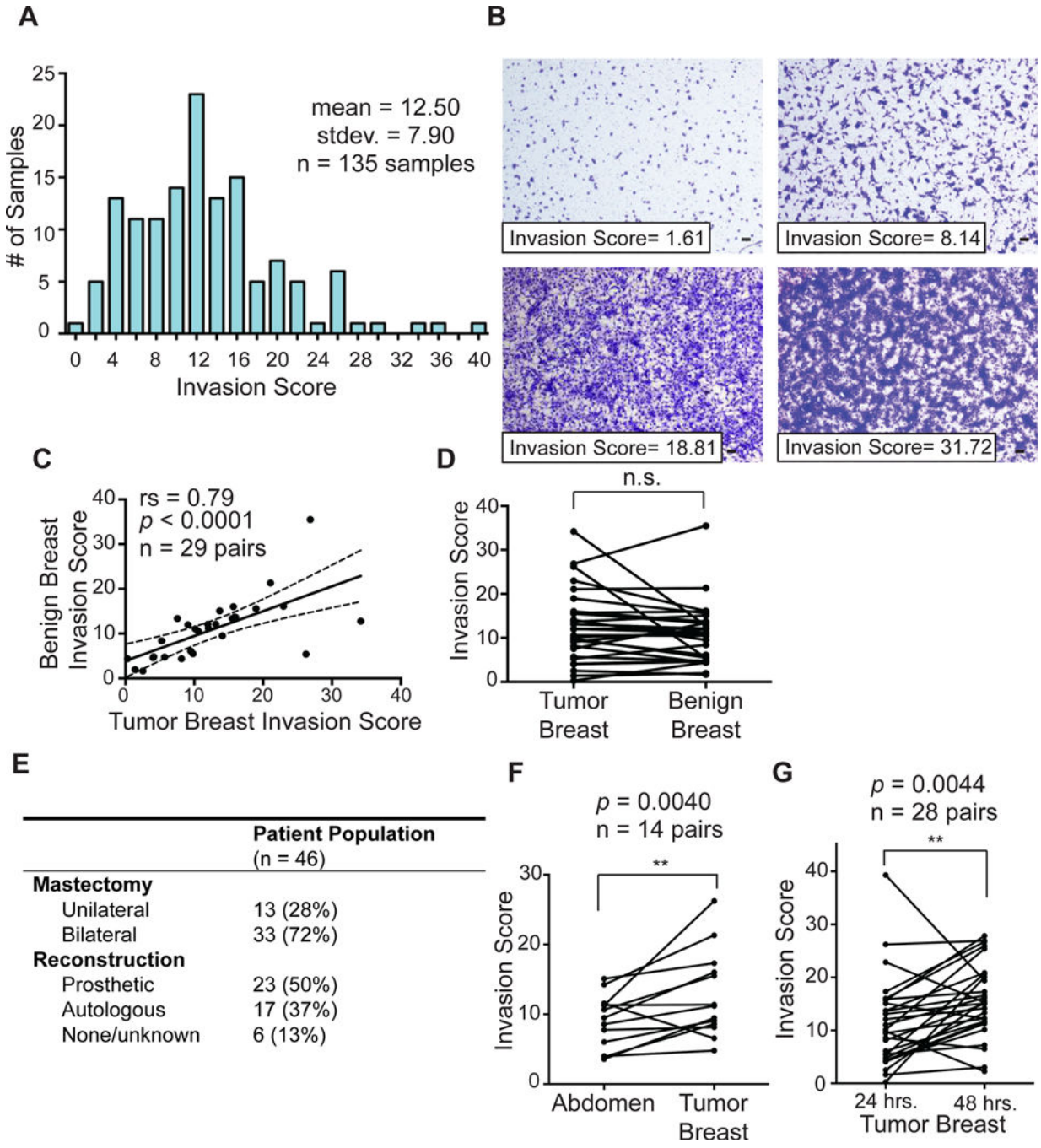

Figure 1.

Classification of PSF according to invasion score identifies patients with high and low score PSF. A) Graph distribution of PSF samples according to calculated invasion score. Histogram of all breast and abdomen PSF samples collected 24 and 48 hours post-mastectomy (mean = 12.503; standard deviation = 7.899; n = 76 samples). B) Representative images of invasion assay of PSF with the indicated invasion score, scale bar = 100 μm. C, D) Comparison of the invasion scores of PSF from the benign and diseased-breasts bilateral mastectomy patients. Invasion scores were treated as a continuous variable, Wilcoxon

matched-pairs signed rank test and linear regression was performed. E) Table of surgery characteristic in the patient population. F) Comparison of the invasion score of individual autologous reconstruction patients from the diseased-breast and abdomen-derived PSF. Invasion scores were treated as a continuous variable, Wilcoxon matched-pairs signed rank test and linear regression was performed. G) as in F but between the same breast from the same patient at 24 and 48 hours after surgery.

A

	Patient Population (n = 46)
Median Age (yr)	49.5 (41.75-55.25)
Menopausal status	
Pre	29 (63%)
Peri	2 (4%)
Post	15 (33%)
Axillary Surgery	
SLN Biopsy	41 (89%)
Completion ALND	13 (28%)
Body Mass Index	27 (23.0-31.0)
Pathologic T stage	
Tis	14 (31%)
T1	20 (43%)
T2	10 (22%)
T3 / T4	0 (0%)
Prophylactic	2 (4%)
Histology	
Ductal	33 (75%)
Lobular	7 (16%)
Both	4 (9%)
Nuclear grade	
Low	3 (7%)
Intermediate	18 (41%)
High	18 (41%)
Not reported	5 (11%)
Median path size (cm)	1.3 (1.03-2.1)
Focality	
Focal	34 (77%)
Multifocal	10 (23%)
Hormone receptor status	
ER+	34 (77%)
ER-	8 (18%)
ER unknown	2 (5%)
PR+	31 (70%)
PR-	11 (25%)
PR unknown	2 (5%)
HER2/Neu receptor status	
HER2/Neu +	3 (7%)
HER2/Neu -	33 (75%)
HER2/Neu not tested	8 (18%)
LVI present	12 (27%)
Positive SLN	13 (30%)

B

Surgical Fluid Collection	Patient Population (n = 46)
Mastectomy samples	
24 hrs. post-op. only	29 (63%)
24 & 48 hrs. post-op.	16 (35%)
48 hrs. post-op. only	1 (2%)
Abdomen samples	
None	31 (67.5%)
24 hrs. post-op. only	8 (17.5%)
24 & 48 hrs. post-op.	6 (13%)
48 hrs. post-op. only	1 (2%)

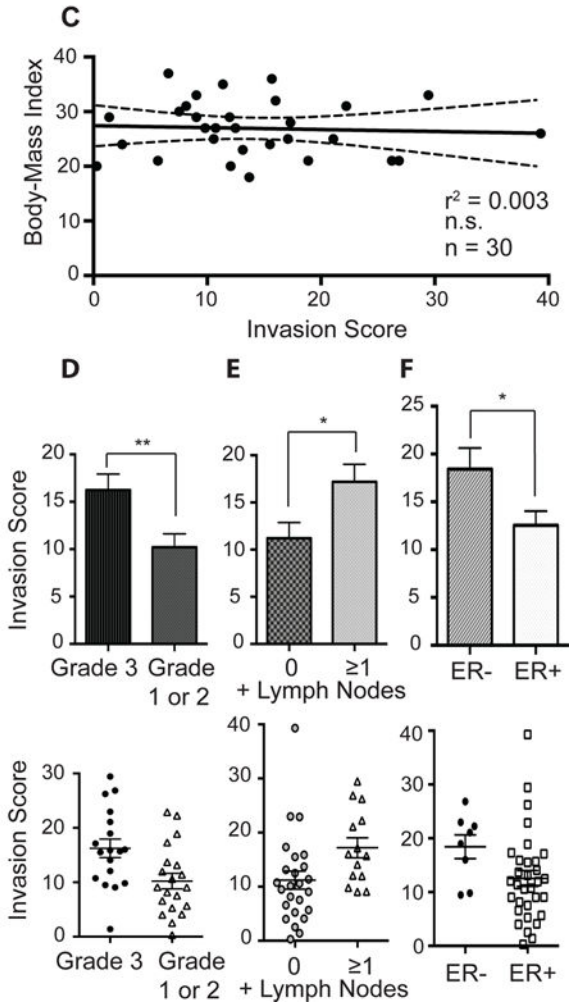

Figure 2.

Retrospective analysis of breast cancer patients reveals correlation between high score PSF and prognostically worse characteristics of primary breast cancers. A) Clinicopathological characteristics of 46 women treated with bilateral or unilateral mastectomy for breast cancer or known BRCA1/2 mutations. Sentinel lymph node (SLN); axillary lymph node dissection (ALND); estrogen receptor (ER); progesterone receptor (PR); human epidermal growth factor receptor 2 (HER2/Neu); Lymphovascular invasion (LVI). B) PSF was collected from the mastectomy and abdominal drains, when possible, 24 and/or 48 hours after surgery. Post-

operatively (post-op.). C) Correlation between body-mass index and invasion scores. ($p = 0.7577$; $n = 30$; $r^2 = 0.003454$; Linear regression). D) Comparison of the invasion scores of all patients with grade 1 and 2 or grade 3 tumors at diagnosis. Invasion scores were treated as a continuous variable, Wilcoxon matched-pairs signed rank test and linear regression was performed. ($p = 0.0071$; Grade 1 or 2, $n = 20$; Grade 3, $n = 18$; Mann-Whitney test). E) Comparison of the invasion score of all patients with lymph node status at diagnosis. Invasion scores were treated as a continuous variable, Wilcoxon matched-pairs signed rank test and linear regression was performed. ($p = 0.0100$; 0 + lymph nodes, $n= 25$; ≥1 + lymph node, $n = 13$; Mann-Whitney test). F) Comparison of the invasion score of all patients with estrogen receptor status at diagnosis. Invasion scores were treated as a continuous variable, Wilcoxon matched-pairs signed rank test and linear regression was performed ($p = 0.0247$; ER+, $n= 32$; ER-, $n = 8$; Mann-Whitney test).

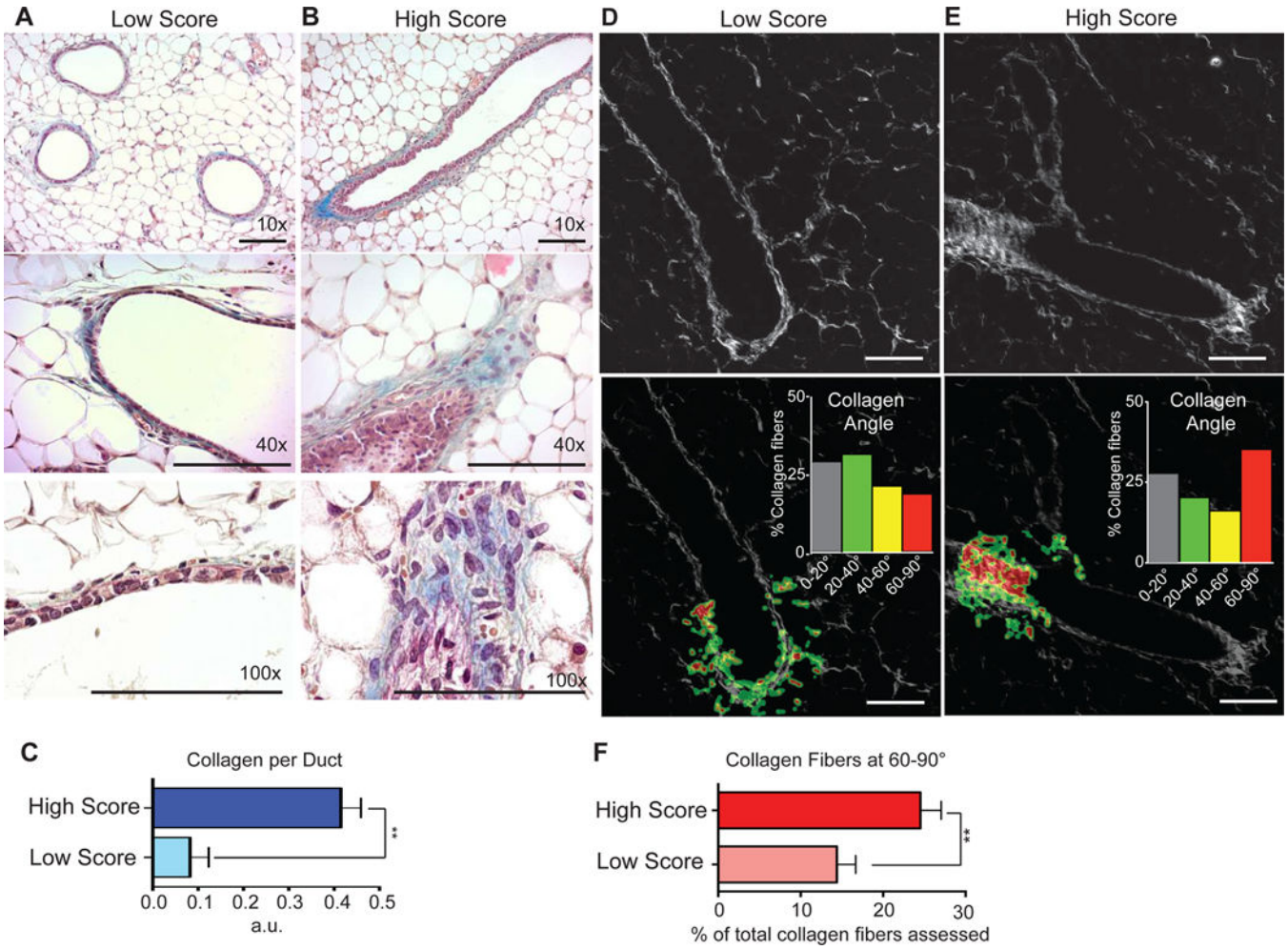

Figure 3.

Exposure of normal mammary gland to high invasion score PSF promotes hyperplasia, collagen deposition, and formation of tumor associated collagen signature 3 (TACS3). A) H&E and Masson's Trichome stain of mammary gland exposed to 1% low score PSF. B) H&E and Masson's Trichome stain of mammary gland exposed to 1% high score PSF. C) Quantification of collagen staining ($p = 0.0032$; n = 3 low score, n = 4 high score, Unpaired t-test with Welch's correction). D) Second harmonic generation imaging and CurveAlign software analysis of mammary ducts exposed to low or high score PSF. (scale bar = 100μm). E) The same was done for high score PSF treated mammary glands identifying the majority of collagen fibers interacting with the ductal border at 60–90°, the empirical definition for TACS3 conformation (scale bar = 100μm). F) Quantification of TACS3 in mammary glands exposed to low and high score PSF ($p = 0.0163$; n = 4 low score, n = 7 high score, Unpaired t-test with Welch's correction).

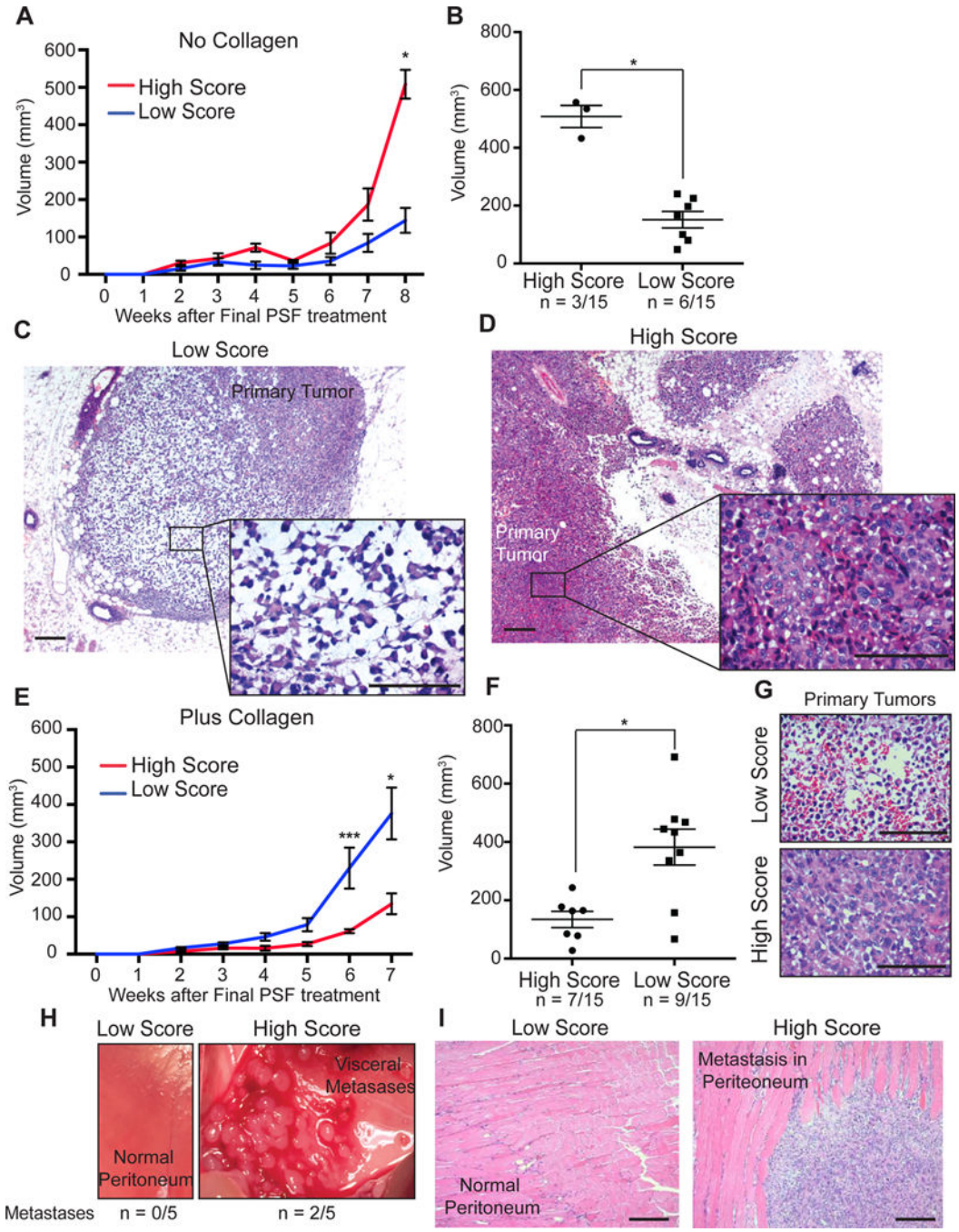

Figure 4.

High score PSF promotes tumor growth, local invasion, and visceral metastasis in the mammary fat pads of nude mice. A) Graph of tumor volume of xenografts of MDA-MB-231 cells were injected in mammary fat pads of nude mice and treated with low or high score PSF in the absence of collagen (Mean ± SEM). B) Tumor volumes at week 8 of experiment described in A. ($p = 0.0167$; High, n = 3; Low, n = 7; Mann Whitney test). C) H&E of representative xenograft from the low score PSF group from experiment in A (scale bar = 100μm). D) H&E of representative xenograft from the high score PSF group (scale bar =

100μm). E) Graph of tumor volume of xenografts of MDA-MB-231 cells injected in mammary fat pads of nude mice and treated with low or high score PSF in presence of collagen (Mean ± SEM) (6 weeks, p = 0.0006; 7 weeks, p = 0.0401; Low, n = 8; High, n = 7; Mann Whitney test). F) Tumor volumes at week 7 of experiment described in E (Mean ± SEM) (p = 0.0229; High, n = 7; Low, n = 9, Mann Whitney Test). G) H&E of representative xenograft from the low score PSF group from experiment in E (scale bar = 100μm). H) Image of a representative peritoneum of mouse treated with low and high score PSF (Metastasis observed in 0/5 mice treated with low score PSF and 2/5 mice treated with high score PSF) I) H&E of a representative peritoneum of mouse treated with low and high score PSF (scale bar = 100μm).

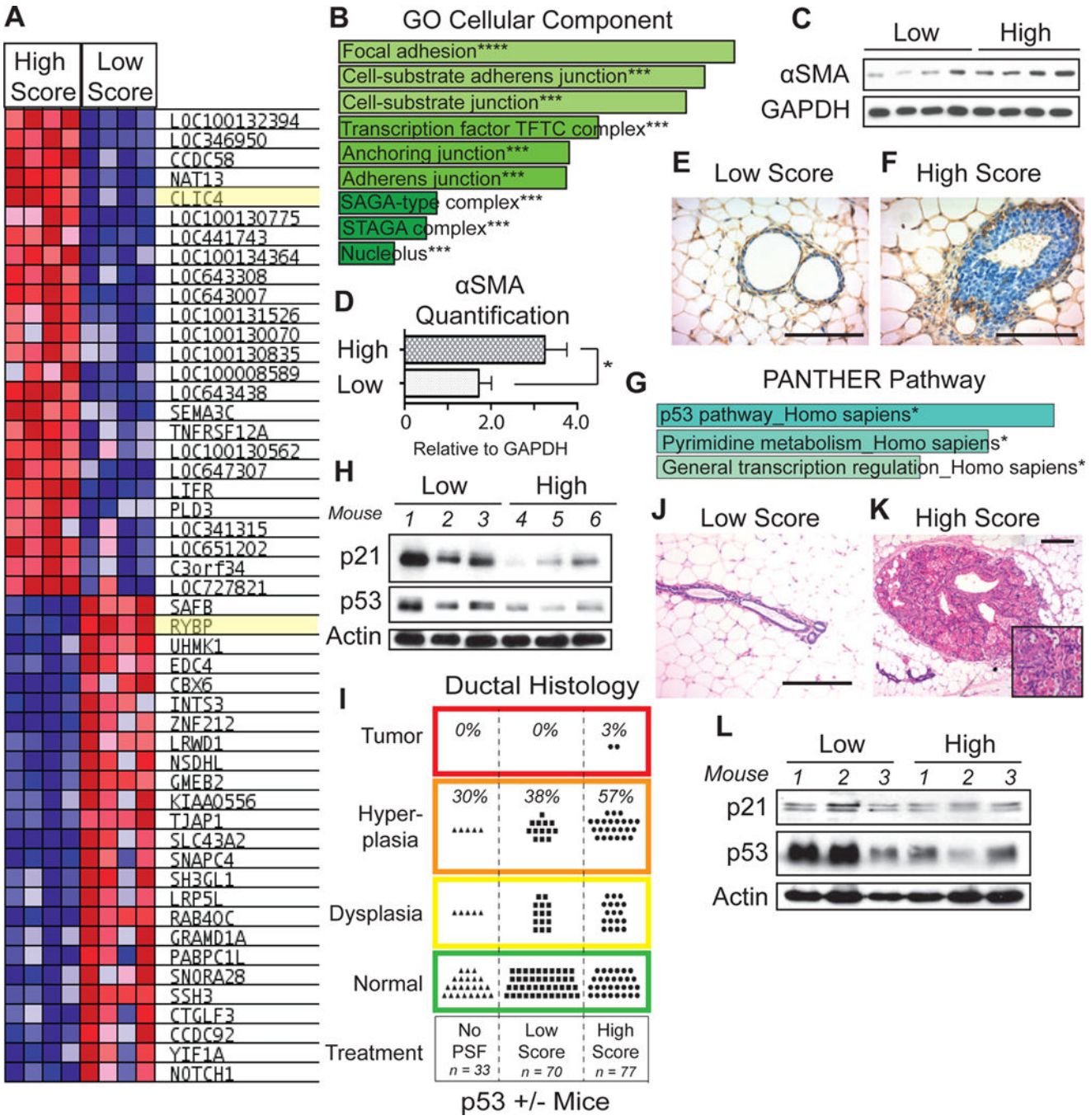

Figure 5.

Identification of chloride intracellular channel 4 (CLIC4) and RYBP as mediators of the effects of high score PSF. A) Gene expression signature of 50 most differentially expressed genes derived from MDA-MB-231 cells treated with 4 different high and 4 different low PSF samples. B) The 1000 most differentially expressed genes between high and low score treated samples were analyzed by Enrichr. GO Cellular Component Ontology identified focal adhesion, cell substrate adherens junction, and cell-substrate junction as the pathways most significantly associated with the differentially expressed genes upon high and low

score treatment (*** $p < 0.001$). C) Western blot analysis of alpha smooth muscle actin (αSMA) as a marker of myofibroblast differentiation in primary human mammary fibroblasts treated with high or low score PSF. D) Quantification of αSMA in C. (Mean ± SEM)($p = 0.0411$, High, n =4; Low, n = 4, Unpaired t-test). E–F) Immunohistochemistry of αSMA in mammary glands of nude mice treated with high or low score PSF. (scale bar = 100μm). G) The 1000 most differentially expressed genes between high and low score treated samples were analyzed by Enrichr. PANTHER Pathway identified the p53 pathway as the pathway most significantly associated with the differentially expressed genes upon high and low score treatment. (* $p<0.05$) H) Western blot analysis of p21 and p53 in mammary glands of nude mice treated with low and high score PSF. Actin was used as the loading control. I) Ductal histology analysis of mammary glands of p53515A/p53WT heterozygous mice untreated with PSF, or treated with high or low score PSF. Treated mice were treated bilaterally with high or low score PS. (n = 5 mice; n = 10 mammary glands per high or low score PSF treatment). J) H&E of a representative mammary gland from p53515A/p53WT heterozygous female mouse treated with low score PSF (scale bar = 100μm). K) H&E of a representative tumor in the mammary gland of a p53515A/p53WT heterozygous female mouse treated with high score PSF (scale bar = 100μm). L) Western blot analysis of p21 and p53 in the mammary gland of p53515A/p53WT heterozygous female mice treated with low and high score PSF.

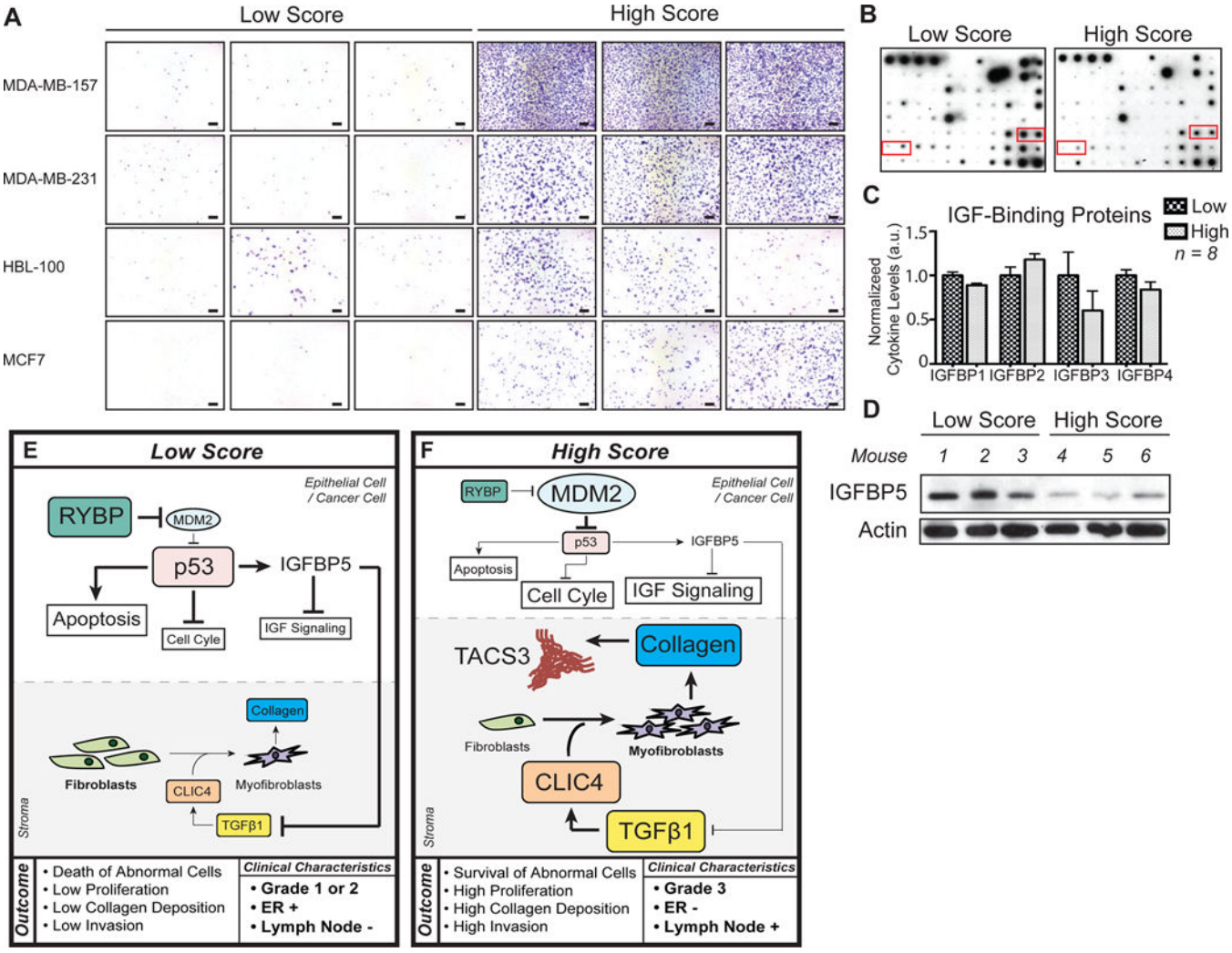

Figure 6.

Invasion inducing capacity of low and high score PSF is maintained across cell lines and correlates with reduction in IGFBP. A) Invasion assays were performed on the indicated 4 cell lines using low and high score fluids from three different patients in each case (scale bar = 100μm). B) Cytokine array exposed to high and low score PSF. The red boxes indicate the positions of IGFBP 1, 2, 3,and 4 on the array. C) Quantification of IGFBPs from cytokine array normalized to positive control (Mean ± SEM) 8 different patient samples were used for analysis (High, n = 4; Low, n = 4). D) Western blot analysis of IGFBP-5 in mammary glands of nude mice treated with different low and high score PSF. Actin was used as a loading control. (n = 6 mice treated separately; High, n = 3; Low, n = 3). E, F) Model of the mode of action of low and high score PSF, respectively. See text for details.